



SEISMIC BEHAVIOR OF LONG PERIOD STRUCTURES SUBJECTED TO NEAR-FAULT EARTHQUAKES

S. F. Ghahari¹, A. R. Khaloo² and P. Ghaderi³

ABSTRACT

Recorded accelerograms in regions near the fault, which are located in the direction of rupture propagation; have specific characteristics such that inclusion of their effects on the response of the structures is necessary. Specially, fling-step, directivity and high frequency content of these records are important. In this paper, the response of 10, 20, 30 and 40 story steel structures designed considering near fault parameters and based on UBC97 regulations is investigated under artificial pulses produced by directivity effect. Despite past studies, it is shown that a long period structure is the one having a ratio of the first mode period to pulse period greater than 0.44. Furthermore, the effect of variations in the pulse period of near fault velocity records on the characteristics of inelastic response of structures is examined. Consequently, analysis of the structures experiencing actual near fault records indicates that the response spectrum obtained from artificial pulses presents the behavior of the structure under actual near fault earthquakes rather accurately.

Introduction

After the Northridge and Kobe earthquakes and because of damage and decimation in urban areas whose structures were designed based on modern seismic codes, the matter of near-field earthquakes was again put in the limelight and extensive studies were conducted in this field, which can be found in new revisions of ATC 40 (1996), FEMA273 (1997), JRA (1996), UBC97 (1997) and FEMA 302 (1998) documents (McRae et al. 2001). After the 1971 San Fernando earthquake, specific response of a structure to a sever pulse recorded near the epicenter was first studied (Mahin et al. 1976; Bertero et al. 1978). They showed that Olive View Medical Center had experienced large damage resulting from an intensive pulse type excitation, which is one of the near-field earthquake characteristics, and concluded that the resultant damage from a few displacement cycles with long amplitude (near-field earthquake) is greater than the damage from more cycles but short amplitude (far-field earthquakes). After 1979 Imperial Valley earthquake, Anderson and Bertero addressed the sensitivity of inelastic response of structures as a function of its strength and the ratio of structural period to the period of dominant pulse in the record. They also suggested that the shape of design spectrum in the range of long period structures should be modified against the pulse type ground motions (Anderson and Bertero 1978). Hall et al. used the wave propagation theory to study the response of a shear building under a pulse type excitation. They warned about destructive effects of near-field earthquakes and insufficiency of existing codes (Hall et al. 1995).

¹ Graduate Student, Dep. of Civil Engineering, Sharif Univ. of Tech., Tehran, Iran.

² Professor, Dep. of Civil Engineering, Sharif Univ. of Tech., Tehran, Iran.

³ Graduate Student, Dep. of Civil Engineering, Sharif Univ. of Tech., Tehran, Iran.

Iwan used a similar elastic structure to obtain the spectrum of drift as a criterion for seismic demand of multi degrees of freedom structures under near-field records. He showed that even for the structures with elastic behavior, near-fault effects cannot be considered in design only with multiplying a single factor in base shear as in UBC97 (Iwan 1997). Alavi and Krawinkler have studied the effects of near-field earthquakes on behavior of frame structures and suggested that these effects are greater for long period structures (Alavi and Krawinkler 2001). Kalkan and Kunnath showed that demands in the fundamental and higher modes must be evaluated by taking into consideration the fact that modal periods shift to the right of the spectrum as the system moves from the elastic to inelastic state (Kalkan and Kunnath 2006).

Input Excitation

To study the structure's response under pulses with different periods, artificial ground motions have been used. For this purpose, because pulse has a deterministic behavior, and background record is a stochastic phenomenon, different models have been suggested for the velocity pulse of near-field earthquakes (Alavi and Krawinkler 2000; Agrawal and He 2002; Menun and Fu 2002; Mavroeidis and Papageorgiou 2003; Xin-Le and Xi 2004; Bray and Rodriguez-Marek 2004). All of these models have two types of error in comparison with real records. First, background records with high frequency content are ignored, therefore some error will occur in structures' response which in some cases can be influential (Ghahari et al. 2006). Secondly, due to of the difference between real and artificial pulse, some error will enter the model. All models presented heretofore include the first type of error and decrease the second effect as much as possible. In this paper, the model proposed by Mavroeidis and Papageorgiou (2003) has been used to mathematically express the pulse. Mathematical equation of its velocity record is as follows:

$$v(t) = A \frac{1}{2} \left[1 + \cos \left(\frac{2\pi f_p}{\gamma} (t - t_0) \right) \right] \cos \left[2\pi f_p (t - t_0) + v \right] \text{ for } t_0 - \frac{\gamma}{2f_p} \leq t \leq t_0 + \frac{\gamma}{2f_p} \quad (1)$$

In which γ , f_p , A and v show number of cycles, pulse frequency, pulse amplitude and phase, respectively. t_0 shows the time of pulse initiation. γ is a number between 1 and 3 and in this paper is 2. This value is based on the results in reference 15. v is used for better fitness of pulse on real record and in this study, its value is zero.

For different records, A has a value close to record's PGV. several equations based on magnitude and distance are presented for PGV (Alavi and Krawinkler 2000; Xin-Le and Xi 2004; Bray and Rodriguez-Marek 2004). Since A is related to Δu (rise velocity in fault), and since Δu is equal to the ratio of rise displacement to rise time (τ) and both of them are functions of rupture specified length (L), hence A is independent of L and as a consequence independent of magnitude. A has a value between 70 to 130 cm/s and therefore a value of 100 is a good approximation (Mavroeidis and Papageorgiou 2003).

The last parameter used as a control variable in this paper, is pulse period (T_p) which is the inverse of pulse frequency. This parameter is a function of rise time and is in direct relation with magnitude. Such as PGV, many equations are presented for the relation of pulse period and magnitude (Alavi and Krawinkler 2000; Mavroeidis and Papageorgiou 2003; Xin-Le and Xi 2004; Bray and Rodriguez-Marek 2004). The Proposed relation by Mavroeidis and Papageorgiou (2003) is:

$$\text{Log}T_p = -2.9 + 0.5M_w \quad (2)$$

In which, T_p is in second and M_w shows the magnitude. Since the main purpose of this paper is to study the effects of T_p variations, the range of 0.5 to 5 seconds with steps of 0.5 is used. According to Eq. 2, this range includes magnitudes between 5.2 and 7.2. Fig. 1 demonstrates time history graphs of all artificial pulses. For comprehensive study, 4 pulses with periods equal to 0.89, 1.89, 2.67 and 3.64, respectively, are also used, which include first mode periods of structures under study.

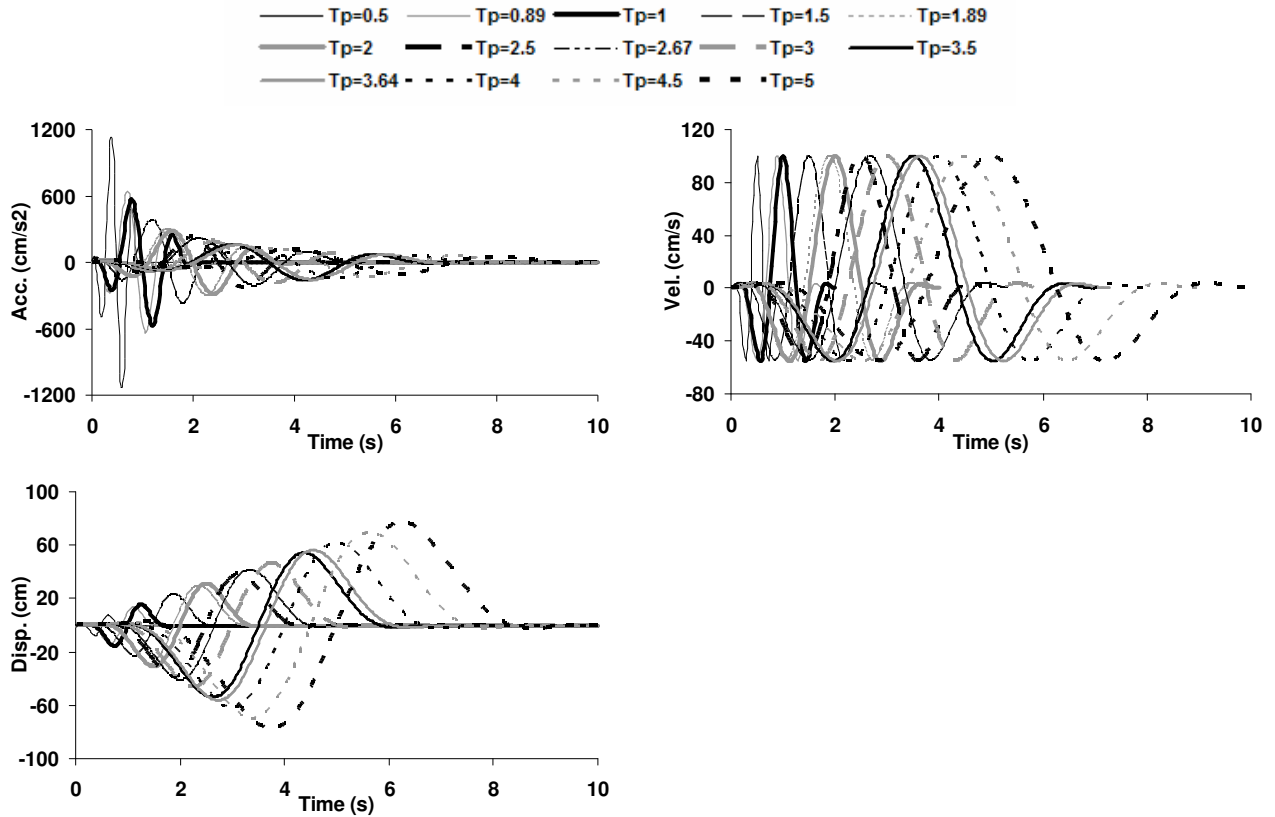


Figure 1. Acceleration, Velocity and Displacement Graphs of Artificial Pulses.

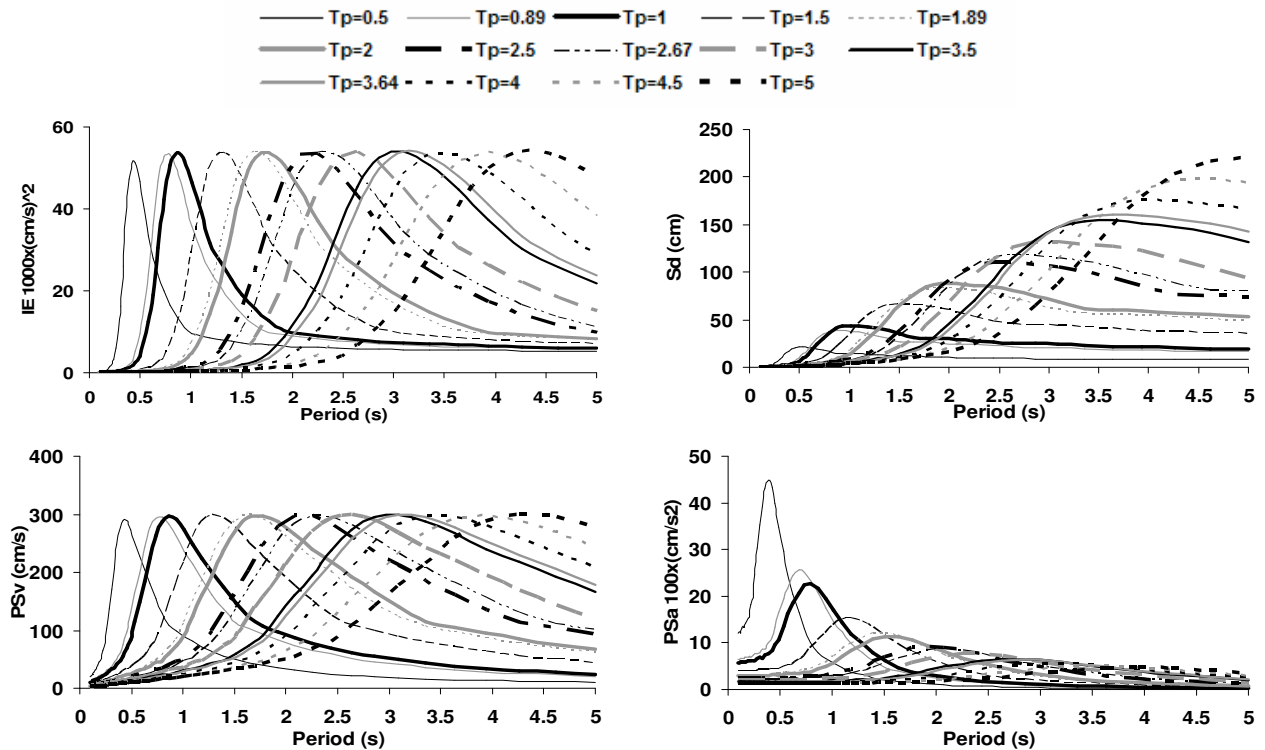


Figure 2. Input Energy, pseudo acceleration, pseudo velocity and displacement Spectrum of artificial pulses.

It can be seen that, as the pulse period (magnitude) increases, the maximum acceleration would decrease and record duration would increase. Velocity amplitude is assumed constant (100 cm/s) and displacement amplitude increases.

Fig. 2 shows the elastic response spectrums of these artificial pulses. The spectrum of input energy shows that maximum values of all records are equal. It also shows that the record exerts more energy to the structure whose period is equal to pulse period. Pseudo acceleration response spectrum shows that short structures if excited under pulses with short period, will be exposed to high accelerations; however such status is not observed in tall structures even under pulses with the same period.

Response of Structures

Figs. 3-a to 3-d are presented to show how the shear forces are distributed along height under pulses with different periods. In these graphs maximum story shear forces have been scaled to total frame weight. In order to compare with design mode, the amount of design shear forces is also provided for both static and spectrum distribution methods. Fig. 3-a shows that shear force distribution for the 10 story structure is non-uniform under pulses with periods less than one second. In the height of 0.6 to 0.8, there is a sudden increase in shear forces (especially for pulse period equal to 0.5 second). Furthermore, maximum shear forces of upper stories are for pulse period of 0.5 second while maximum shear forces of lower stories pertain to one second pulse period.

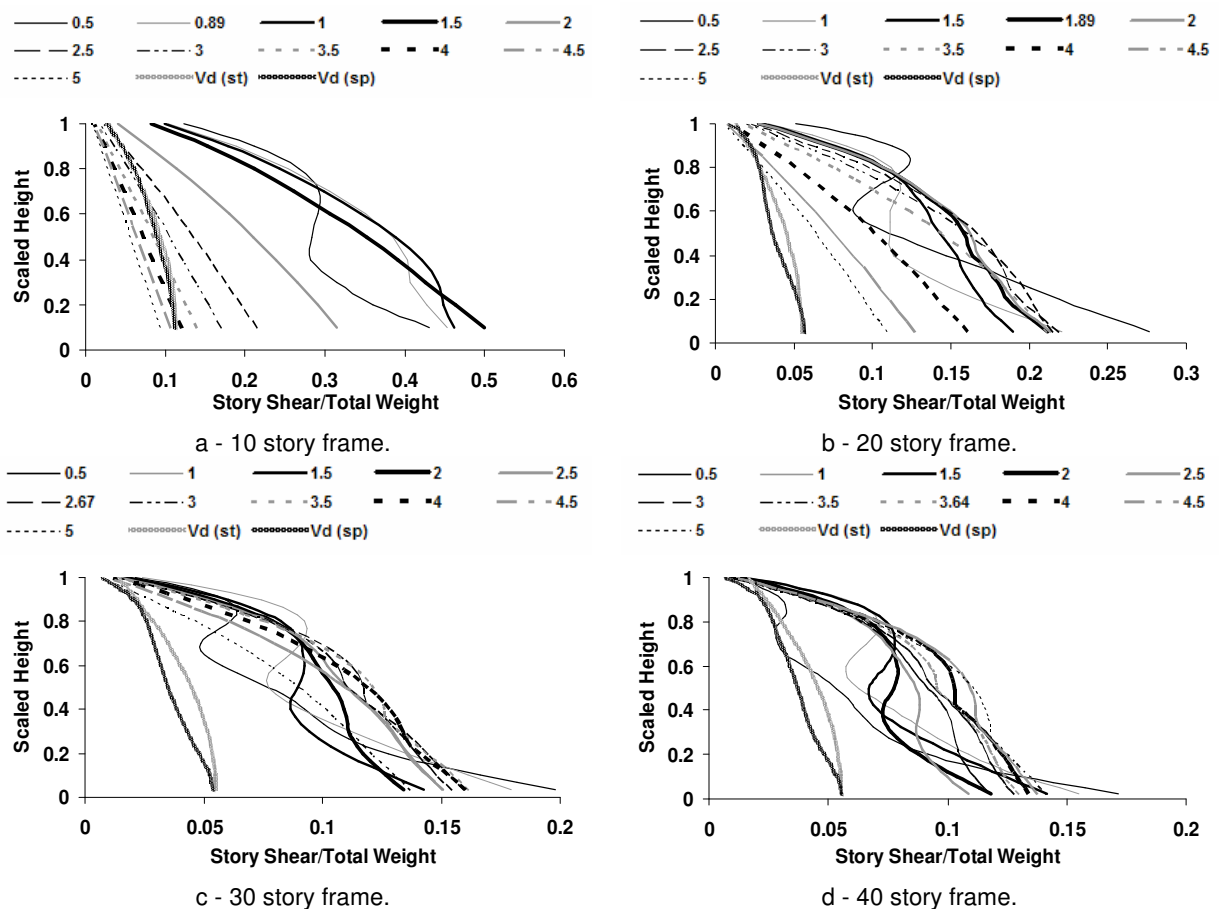


Figure 3. Shear forces distribution of frames for different pulse periods along with design shear forces.

Fig. 3-b shows that shear forces distribution for the 20 story structure is non-uniform under pulses with periods less than two seconds. In the height of 0.7 to 0.9, there is a sudden increase in shear forces

(especially for pulse period equal to 0.5 and 1 second). Furthermore, maximum shear forces of upper stories are for pulse period of 0.5 second while for mid stories pertain to 2.5 second pulse period and maximum shear forces of lower stories are again for pulse period of 0.5 second. In 30 and 40 story structures distribution of shear forces for all pulse periods is non-uniform (Figs. 3-c and 3-d). To find the value of T/T_p after which structure is considered a long period structure, we'd better draw the shear force distribution graphs for each pulse period, separately. Fig. 4 shows these graphs.

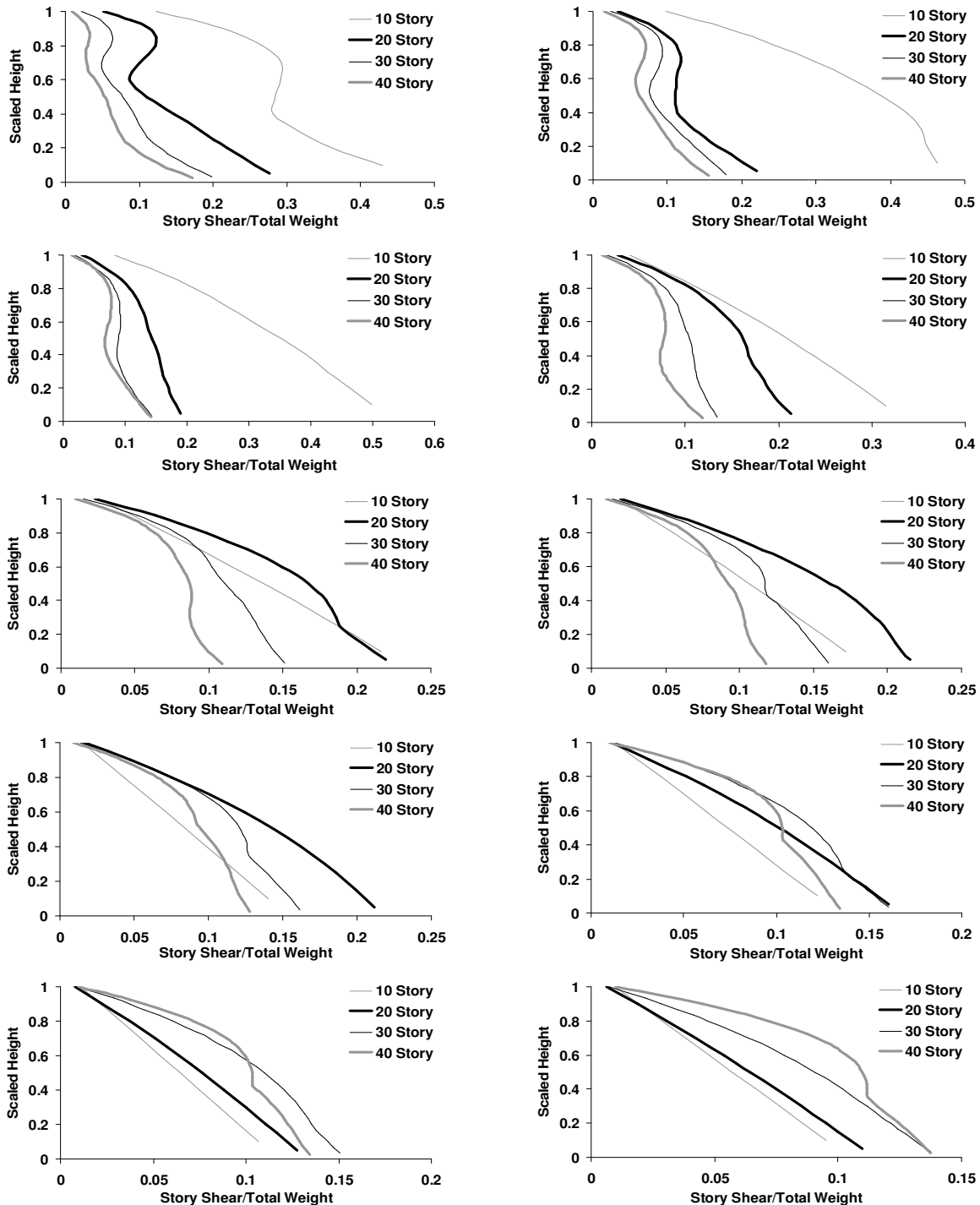


Figure 4. Story shear distribution under different pulses. Graphs from left to right and from up to down respectively show pulses with periods equal to 0.5, 1, 1.5, 2, 2.5, 3, 3.5, 4, 4.5 & 5 seconds.

It can be seen that, in the shortest pulse period (0.5 second), the 10 story structure is affected more than the others, followed by 20, 30 and 40 story structures. With increase in the pulse period, short structures are respectively replaced by taller structures and each structure has a triangular uniform distribution for pulse periods greater than a specific value. This can be clearly seen for 10 and 20 story structures. However, due to limited number of analysis, this is not observed for 30 and 40 story structures. This pulse period is equal to 2 for the 10 story structure and to 4.5 for the 20 story structure. Dividing the 10 story structural period to 2 and the 20 story structural period to 4.5 results in 0.44 and 0.42. So, structures are considered long period when their T/T_p ratio are greater than 0.44. This pulse period for 30 and 40 story structures will be equal to 6 and 8.27 seconds, respectively.

Figs. 5-a to 5-d show the scaled inter-story displacement (drift) graphs for different structures. Fig. 5-a shows that for the 10 story structure, drift distribution for pulse periods less than 2 seconds is greatly non-uniform and in upper stories, higher than 0.3 of structural height, values increase rapidly. A pulse period of 1.5 second shall produce a great sudden drift in the first story of the 10 story structure. In no case, drift is greater than the allowable value of 0.02.

Fig. 5-b shows the same graphs for the 20 story structure. The results are not similar to the 10 story structure. However, the drift is again greater in upper stories. Maximum drift is related to 2.5 second pulse period which is greater than the allowable value.

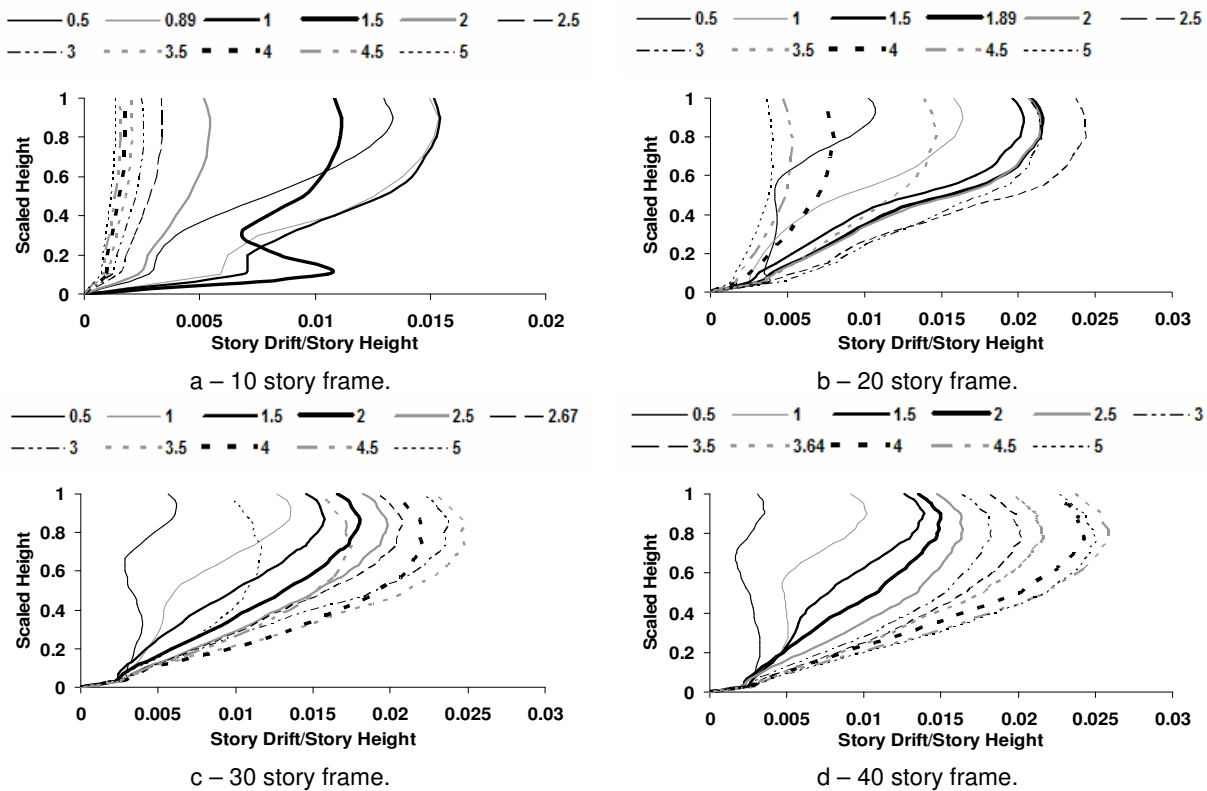


Figure 5. Scaled Inter-story displacement distribution graphs of structures for different pulse periods.

Fig. 5-c shows that the 30 story structure will have the maximum drift in upper stories, for the 3.5 second pulse period and in lower stories, for 4 second pulse period. The 40 story structure behaves similar to 20 and 30 story structures, however the pulse period corresponding to the maximum drift in upper and lower stories are 4.5 and 5, this is shown in Fig. 5-d.

Fig. 6 shows calculations that were performed in Fig. 4 for shear force distribution. It can be seen that the trend is similar to shear forces and increase in pulse period, the structures order will be reversed.

However, this will occur more rapidly in this case. This shows the higher sensitivity of drift versus pulse period in comparison with shear forces.

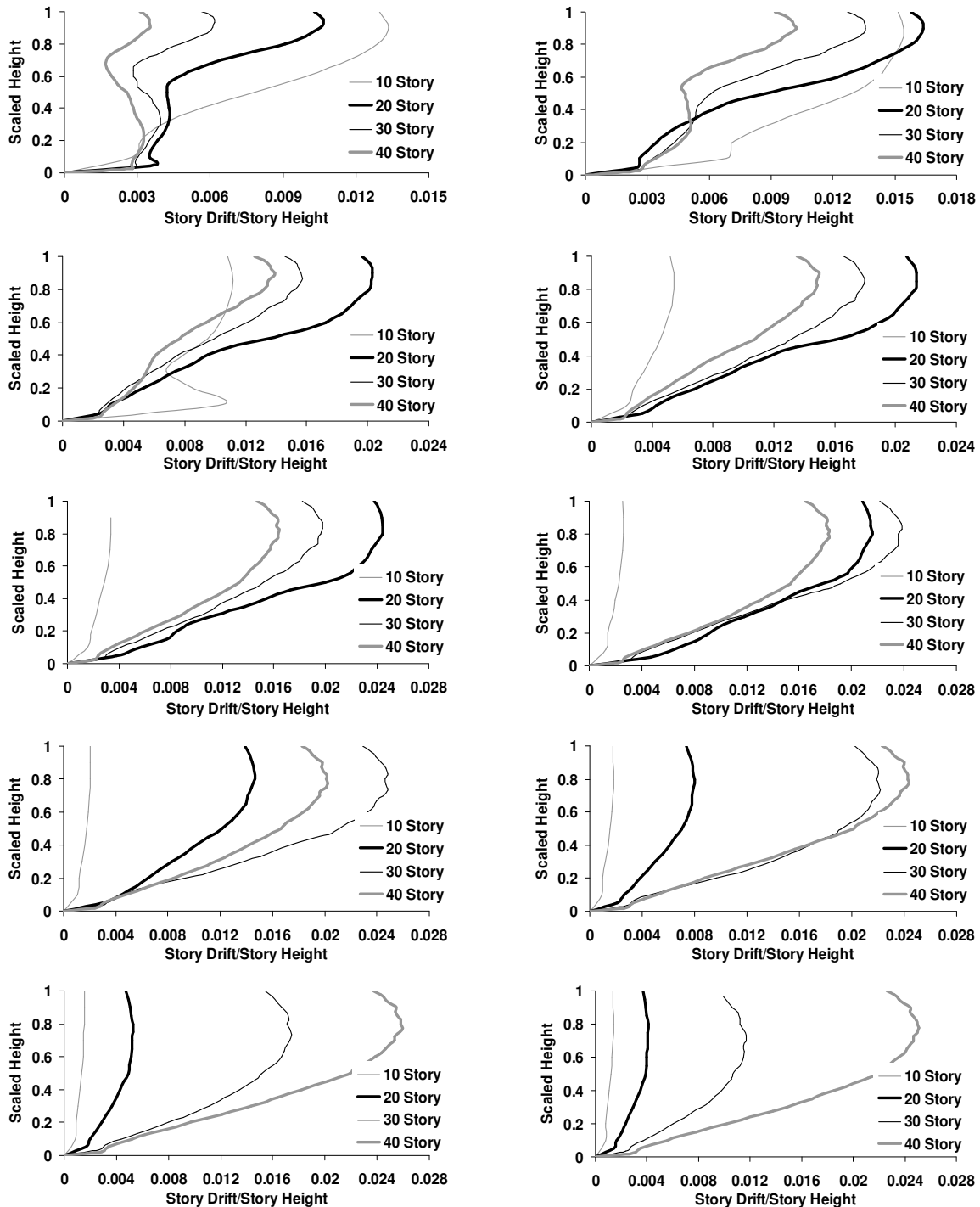


Figure 6. Drift distribution under different pulses. Graphs from left to right and from up to down respectively show pulses with periods equal to 0.5, 1, 1.5, 2, 2.5, 3, 3.5, 4, 4.5 & 5 second.

To generalize the results, they should be presented as spectrums. So, three response spectrums will be presented including base shear, roof displacement and maximum story drift. To compare the structures'

response, each parameter should be scaled with appropriate value such as roof displacement with height of structure etc. Furthermore for a more inclusive study, the horizontal axis is shown as structural period divided by pulse period. Fig. 7-a shows the base shear spectrum. As the height of structure increases, the base shear factor would decrease. The following pattern is similar for all structures: with an increase in T/T_p , the factor increases until it reaches a peak after which it decreases and remains constant. T/T_p for the peak is about 0.6. If the structural period is more than two times greater than the pulse period, the base shear remains constant. Therefore, the range in which T/T_p is effective varies between 0.44 and 2. Below 0.44, base shear decreases rapidly and is independent of the near-field or far-field earthquakes. Fig. 7-b shows the roof displacement spectrum. This graphs show some important results. In all four curves when the T/T_p increases, the trend is upward at the beginning until it reaches to 0.8.

The last response spectrum, which is more deterministic and which expresses a more general rule, is the maximum scaled inter-story displacement or the maximum drift spectrum. Fig. 7-c shows these graphs for the four structures. In this figure the curves are close to each other. Also, this figure shows that the 10 story structure has a different behavior and for structures with periods more than one second (taller than 10 story structures) unique drift response spectrums independent of structure's stories can be presented. From all structures, the structure having T/T_p equal to 0.8 will suffer the greatest displacement under near-field earthquakes.

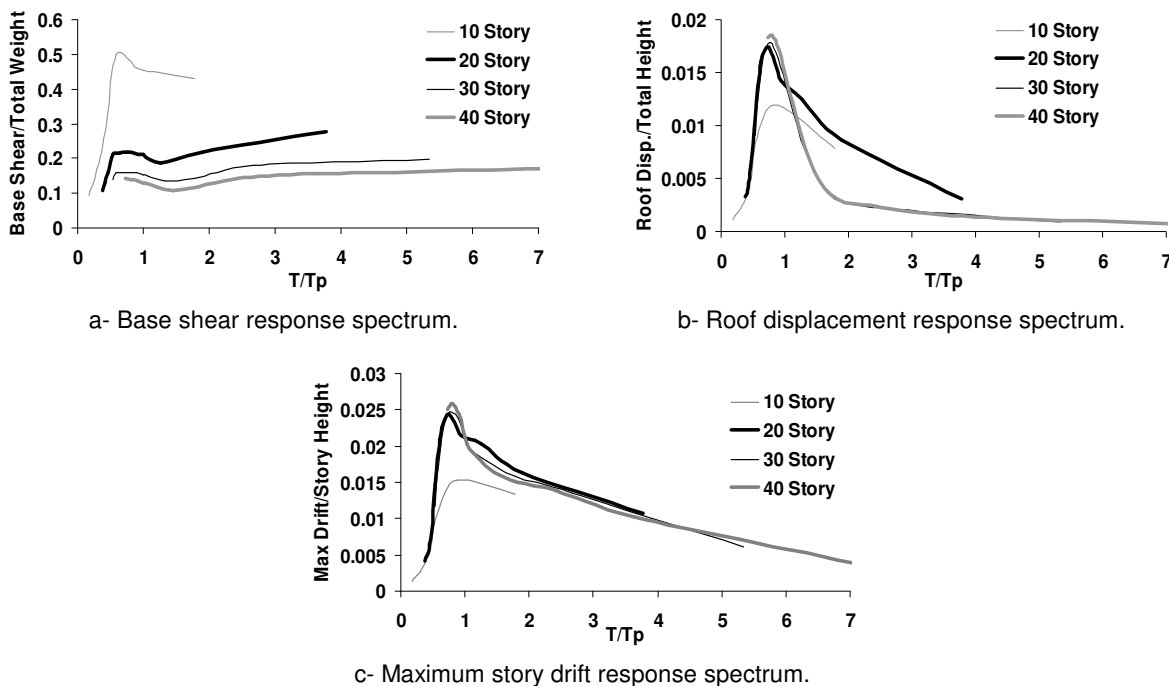


Figure 7. Response spectrums of structures.

In this stage, the responses of aforementioned structures to two actual near-field records are studied and the results are compared with the results obtained from artificial record spectrums to verify their correctness. For this purpose, normal components of the records of Kobe (1995) and Loma Prieta (1989) earthquakes which are recorded in near-field regions with forward directivity are used. Dominant pulse period in records are respectively 0.9 and 3 seconds and their PGV are equal to 160 and 170 cm/s. Table 1 shows the T/T_p values for each structure and earthquake. This table contains an appropriate range for testing the results of Fig. 7. Figs. 8-a and 8-b show roof drift for the structures under two aforementioned earthquakes. Based on Fig. 8 in comparison with curves in Fig. 7-c, following results will be derived:

- a) The 10 story structure in Loma Prieta earthquake shows the lowest response because its T/T_p value is between 0.3 and 2. However, in Kobe earthquake despite Fig. 7-c, the 10 story structure shows an intensive response which can be justified by resonance phenomenon.
- b) 20 and 30 story structures show the most intensive response in Kobe earthquake since their T/T_p value is falls around the peak in Fig. 7-c.
- c) According to upward trend of T/T_p value in 20, 30 and 40 story structures in Kobe earthquake, their response decreases respectively.

Table 1 – T/T_p Values for different earthquakes and different structures.

	Kobe	Loma Prieta
10 story frame	1	0.3
20 story frame	2.1	0.63
30 story frame	2.97	0.89
40 story frame	4	1.21

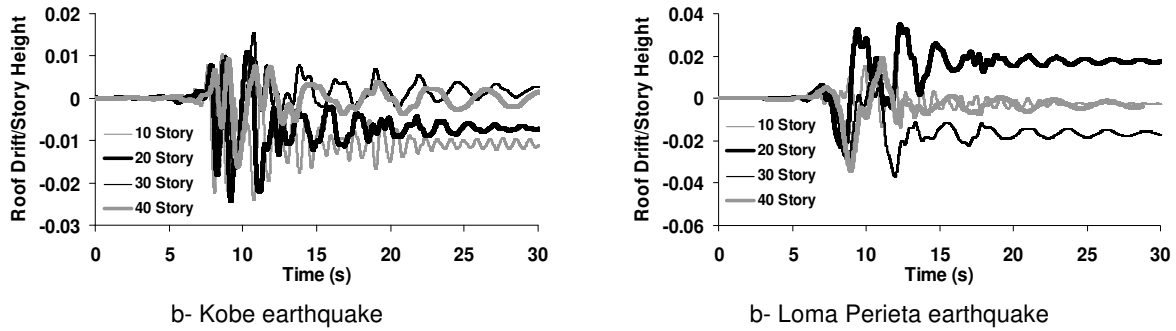


Figure 8. Time History for roof drifts of all structures under Kobe & Loma Prieta earthquakes.

Therefore the results of artificial records and the general rules driven from them can estimate general response of structures under near-field earthquakes satisfactorily. The curve plotted by information in table 1 (points related to response 10 story structure are excluded) is drawn along with Fig. 7-c. This figure shows the mentioned compatibility graphically. The higher response of structures under real record is due to the difference between maximum velocity of artificial records and maximum velocity of real records (Fig. 9).

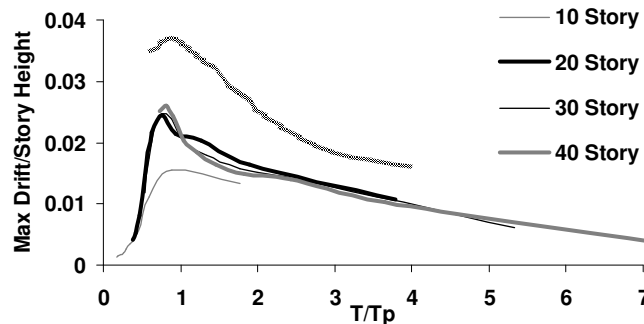


Figure 9. Repeat of Fig. 7-c along with results of real records.

Conclusions

Recorded accelerograms in regions near the fault, which are located in the direction of rupture propagation, have specific characteristics that inclusion of their effects on the response of the structures is necessary. Specially, fling-step, directivity and high frequency content of these records are important. In this paper the response of 10, 20, 30 and 40 story steel structures designed based on UBC97 regulations and considering near fault parameters were investigated under artificial pulses produced by directivity effect. These synthetic velocity pulses have constant amplitudes because PGV is independent of magnitude and variable periods which are function of earthquake magnitude. Response of structures containing shear force and drift distribution showed that despite past studies, a long period structure is the one having a ratio of the first mode period to pulse period greater than 0.44. Furthermore, the effect of variations in the pulse period of near fault velocity records on the characteristics of inelastic response of structures was examined. Results of analysis results show that 10 story structure designed based UBC 97 behaves differently in comparison with other long period structures. Consequently, analysis of the structures experiencing actual near fault records indicated that the response spectrum obtained from artificial pulses presents the behavior of the structure under actual near fault earthquakes satisfactorily. Also, it was shown that maximum roof drift in structures with period near to 0.8 of pulse period is larger than others.

References

- Agrawal, A.K., and W.-L He, 2002. A closed-form approximation of near-fault ground motion pulses for flexible structures, *15th ASCE Engineering Mechanics Conference*, Columbia University, New York.
- Alavi, B., and H. Krawinkler, 2000. Consideration of near-fault ground motion effects in seismic design, *Proceedings of the 12th World Conference on Earthquake Engineering*, Paper 2665.
- Alavi, B., and H. Krawinkler, 2001. Effects of near-fault ground motions on frame structures, *The John A. Blume Earthquake Engineering Center*, Report No.138.
- Anderson, J., and V. Bertero, 1978. Uncertainties in establishing design earthquake, *ASCE Journal of Structural Engineering* 113 (8), 1709-1724.
- Bertero, V., S. Mahin, and R. Herrera, 1978. A seismic design implications of near-fault san fernando earthquake records, *Earthquake Engineering and Structural Dynamics* 6, 31-42.
- Bray, J., and A. Rodriguez-Marek, 2004. Characterization of forward- directivity ground motions in the near-fault region, *Soil Dynamics and Earthquake Engineering* 24, 815-828.
- Ghahari, F., H. Jahankhah, and M.A. Ghannad, 2006. The effect of background record on response of structures subjected to near-fault ground motions, *First European Conference on Earthquake Engineering and Seismology*, Paper No. 1512, Geneva, Switzerland.
- Hall, J., T. Heaton, M. Halling, and D. Wald, 1995. Near-Source ground motion and its effects on flexible buildings, *Earthquake Spectra* 11 (4), 569-605.
- Iwan, W., 1997. Drift spectrum: measure of demand for earthquake ground motions, *ASCE Journal of Structural Engineering* 123 (4), 397-404.
- Kalkan, E., and S.K., Kunnath, 2006. Effects of fling-step and forward directivity on the seismic response of buildings, *Earthquake Spectra* 22 (3), 367-390.

- MacRae, A., D. Morrow, and C. Roeder, 2001. Near-fault ground motion effects on simple structures, *Journal of Structural Engineering* 127, 22188.
- Mahin, S., V. Bertero, A. Chopra, and R. Collins, 1976. Response of the olive view hospital main building during the san fernando earthquake, *Earthquake Engineering Research Center*, University of California, Report No. UCB/EERC-76/22.
- Mavroeidis, G. P., and S. A. Papageorgiou, 2003. A mathematical representation of near-fault ground motions, *Bulletin of the Seismological Society of America* 93 (3), 1099-1131.
- Mavroeidis, G.P., and S. A. Papageorgiou, 2004. Near-Fault ground motions, and the response of elastic and inelastic Single-Degree-Of-Freedom (SDOF) systems, *Earthquake Engineering and Structural Dynamics* 33, 1023-1049.
- Menun, C., and Q. Fu, 2002. An analytical model for near-fault ground motions and the response of SDOF systems, *7th U.S National Conference on Earthquake Engineering*, Mira Digital Publishing No. 00011, Boston, Massachusetts.
- Xin-le, L., and Z. Xi, 2004. Study on equivalent velocity pulse of near-fault ground motions, *ACTA Seismological Sinica* 17 (6), 697-706.